

# Dynamic Rheological Behavior and Morphology of Poly(trimethylene terephthalate)/Poly(ethylene octene) Copolymer Blends

Wei-Ang Luo,<sup>1</sup> Guobin Yi,<sup>2</sup> Jin Yang,<sup>1</sup> Zhengfu Liao,<sup>3</sup> Xudong Chen,<sup>1</sup>  
Kancheng Mai,<sup>1</sup> Mingqiu Zhang<sup>1</sup>

<sup>1</sup>Key Laboratory for Polymer Composites and Functional Materials (Ministry of Education),  
School of Chemistry and Chemical Engineering, Sun Yat-Sen University, Guangzhou 510275, China

<sup>2</sup>Faculty of Light and Chemical Engineering, Guangdong University of Technology, Guangzhou 510006, China

<sup>3</sup>Faculty of Materials and Energy, Guangdong University of Technology, Guangzhou 510006, China

Received 26 May 2008; accepted 2 July 2009

DOI 10.1002/app.31054

Published online 15 September 2009 in Wiley InterScience (www.interscience.wiley.com).

**ABSTRACT:** The dynamic rheology and morphology of poly(trimethylene terephthalate) and maleic anhydride grafted poly(ethylene octene) composites were investigated. A specific viscoelastic phenomenon, that is, a second plateau, appeared at low frequencies and exhibited a certain dependence on the content of elastomer particles and the temperature. This phenomenon was attributed to the formation of an aggregation structure of rubber particles. The analyses of the dynamic viscoelastic functions suggested that the heterogeneity of the composites was

enhanced as the particle content or temperature increased. The microstructural observation by scanning electron microscopy confirmed that maleic anhydride could react with the end groups of poly(trimethylene terephthalate) to form a stable interfacial layer and result in a smaller dispersed-phase particle size due to the reduced interface tension. © 2009 Wiley Periodicals, Inc. *J Appl Polym Sci* 115: 1015–1021, 2010

**Key words:** blending; blends; rheology

## INTRODUCTION

Poly(trimethylene terephthalate) (PTT) was introduced commercially in 1998 by Shell Chemicals under the trade name Corterra. Because of the odd-carbon effect, PTT fiber has high resilience and elastic recovery and can be used in carpet and other textile fiber applications.<sup>1–3</sup> In addition, because of its good physical, chemical, mechanical, and thermal stabilities, PTT has the most competitive predominance in the field of thermoplastic engineering plastics.<sup>4</sup> However, the poor impact strength of PTT at low temperatures limits its applications. Blending is an effective method to obtain new polymeric materials with desired properties and relatively lower cost. The impact properties of PTT can be improved via blending with other elastomers, such as poly(ether imide),<sup>5</sup> ethylene–propylene–diene monomer,<sup>6–9</sup> and poly(ethylene naphthalate).<sup>10,11</sup>

The copolymer poly(ethylene octene) (POE) is a new kind of thermoplastic elastomer with excellent low-temperature mechanical properties. Moreover, maleic anhydride grafted poly(ethylene octene) (mPOE) is an effective toughening agent for polymers. There are some reports about mPOE as a toughener, such as mPOE-toughened poly(ethylene terephthalate) (PET),<sup>12</sup> nylon,<sup>13</sup> and PP.<sup>14</sup> Chiu and Hsiao<sup>12</sup> reported that the notched Izod impact strengths of PET/mPOE were about 5- and 25-fold greater than those of pure PET at 0°C and room temperature, respectively. Recently, an investigation of PTT/mPOE blends was reported.<sup>15</sup> That study mainly focused on the phase structure, morphology, and mechanical properties of the blend system, and the results indicate that the notched impact strength of PTT/mPOE with an mPOE content above 25 wt % was 15-fold greater than that of pure PTT.<sup>15</sup> For high-impact materials obtained by the combination of thermoplastic crystalline polymers with elastomers, factors such as the crystallinity of the matrix, the elastomer content, the size and shape of the dispersed particles, and the interface characteristics have the most important influence on the level of toughening.<sup>16</sup> The interfacial tension<sup>14</sup> and interfacial particle distance<sup>16</sup> are important parameters that control the toughness of a blend system. In brief, the properties of blends strongly depend on the

Correspondence to: X. Chen (cesxcd@mail.sysu.edu.cn).

Contract grant sponsor: Natural Science Foundation of China (to X.C.); contract grant number: 50673104.

Contract grant sponsor: Natural Science Foundation of Guangdong Province of China (to X.C.); contract grant number: 7003702.

structure and morphology of the system, and they are dominantly determined by their rheological characteristics. However, to our knowledge, few results concerning the rheological behavior of PTT/mPOE systems have been reported. Hence, a deep understanding of the rheological properties of PTT/mPOE blends in the molten state is of both theoretical and practical importance.

Dynamic rheology testing is thought to be a preferential method for investigating the structure/morphology of materials because the structure of materials exposed to the testing processes is not destroyed under small-strain amplitude.<sup>17</sup> The rheology and morphology of multiphase polymer blends are strongly affected by interfacial characteristics. Several models have been proposed to describe the phase behavior of binary polymer blends, such as the time-temperature superposition principle,<sup>18–21</sup> Han plots ( $\log G' - \log G''$ , where  $G'$  is the dynamic storage modulus and  $G''$  is the dynamic loss modulus),<sup>18,19,22</sup> and Cole–Cole plots.<sup>20,21,23</sup> The main objectives of this study were to investigate the phase behavior and morphology of PTT/mPOE blends by the dynamic rheological and morphological methods and to determine the effects of the mPOE content and experimental temperature on the rheological properties.

## EXPERIMENTAL

### Materials

PTT, with an intrinsic viscosity of 0.91 dL/g (measured in 60/40 phenol/tetrachloroethane at 298 K), was provided by Shell Chemicals Co. (Guangdong, China). POE with an octene content of 39% (Engage 8150) was supplied by Dupont-Dow (Wilmington, DE) (specific gravity = 0.868 g/cm<sup>3</sup>, melt flow index = 0.5 dg/min). Maleic anhydride (MAH; number-average molecular weight = 98.02 g/mol), purchased from Qifeng Chemical Reagent Factory (Shandong, China), was recrystallized twice with CHCl<sub>3</sub>.

All of the raw materials were dried at 80°C in a vacuum oven 24 h before processing.

### Sample preparation

mPOE was synthesized with a corotating intermeshing twin-screw extruder with a screw configuration adapted for grafting. POE granules and 1.2 wt % MAH were fed to the extruder set at 200°C. The grafting ratio of MAH was about 1 wt %, as determined by quantitative infrared spectroscopy with the adsorption band at 1790 cm<sup>-1</sup>.<sup>24</sup>

All of the blends examined were prepared in an instrumented batch mixer (HBI System 90, Haake, USA) with two counter-rotating roller blades at

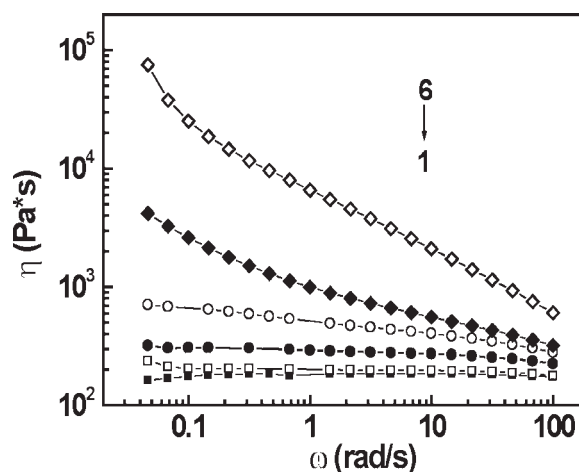


**Figure 1**  $\omega$  dependence of the complex viscosity ( $\eta$ ) for the PTT/mPOE blends at 245°C: (1) 100/0, (2) 95/5, (3) 90/10, (4) 85/15, (5) 80/20, and (6) 0/100 w/w.

260°C and 60 rpm for 5 min. Sheets 2 mm thick were prepared by compression molding at 260°C under 10 MPa.

### Measurement

Scanning electron microscopy (SEM) was performed on a JSM-6330F instrument (Hitachi, Tokyo, Japan) and with an accelerating voltage of 10 kV. The blends samples, including PTT/POE and PTT/mPOE, were cryofractured in liquid nitrogen, and the fracture surface was coated with 10-Å platinum for examination. Before cryofracturing, one of the PTT/mPOE specimens was immersed in xylene solvent for about 48 h at 138°C (its boiling point) to extract the impact modifiers.

The rheological tests were conducted at 200°C on an Advanced Rheometric Expansion System (TA Instruments, New Castle, DE) with parallel plate geometry 25 mm in diameter. The dynamic sweep frequency was from 10<sup>2</sup> to 10<sup>-2</sup> rad/s at 230, 240, 245, 250, and 260°C. A 5% strain amplitude was used to ensure that the rheological behavior was located in a linear viscoelastic range. The steady-rate sweep temperature was 245°C. The parallel gap was 2 mm, and the shear rate range was from 10<sup>-3</sup> to 10<sup>2</sup> s<sup>-1</sup>.

## RESULTS AND DISCUSSION

### Dynamic viscoelastic properties for PTT/mPOE

Figure 1 depicts the dependence of complex viscosity on frequency at 245°C for PTT, mPOE, and their blends, respectively. Generally, the viscosity values decreased as the frequency increased, especially at low frequencies. This could be attributed to the extra stresses connected with the shape relaxation of the droplets of the dispersed phase driven by the interfacial tension.<sup>25,26</sup> As shown in Figure 1, the

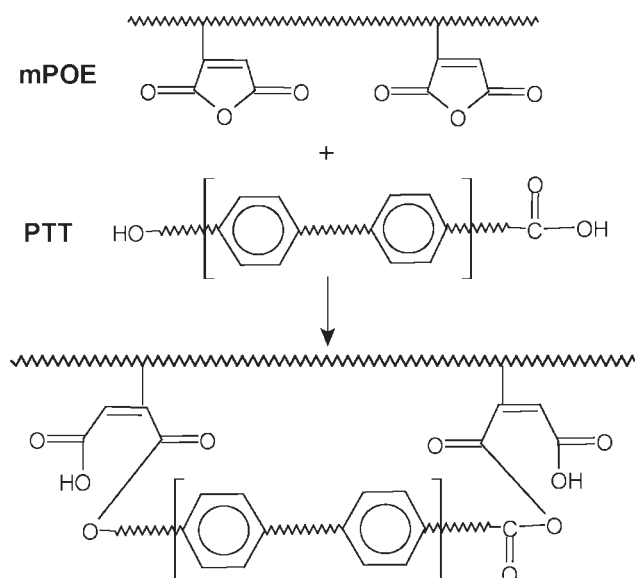


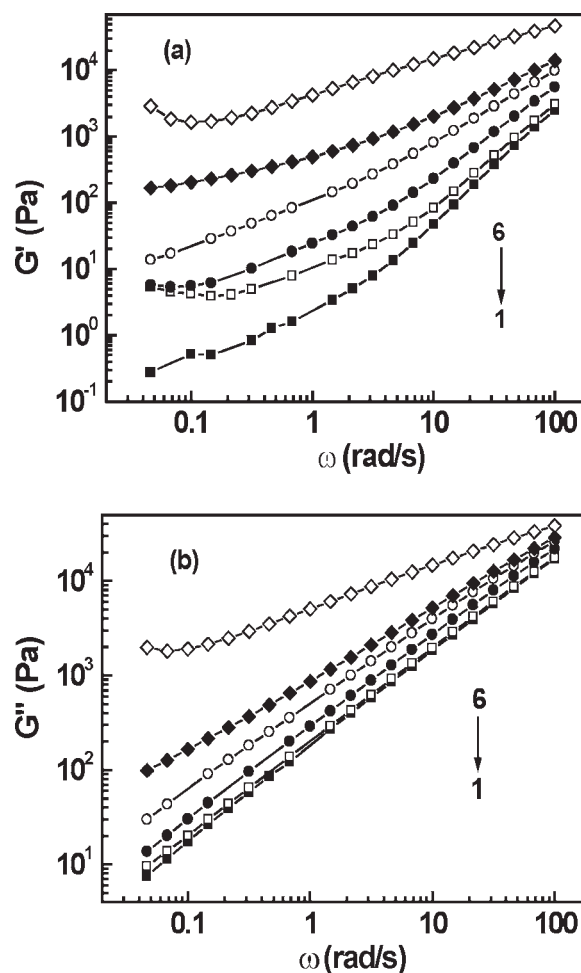
**Figure 2** Possible reaction schemes for PTT/mPOE.

viscosity of the blends was always higher than that of neat PTT but lower than that of pure mPOE. Moreover, the viscosity of the blends increased with increasing mPOE content. This phenomena was ascribed to the effect of entanglement, which was caused by the formation of interchain chemical bonds (see Fig. 2) or the physical entanglement of mPOE chains. As shown in Figure 2, the terminal functional groups of PTT ( $-\text{OH}$  or  $-\text{COOH}$ ) reacted with the MAH side groups of mPOE. The entanglement of chains severely impeded the flow of the melt at low frequencies and consequently led to the higher viscosity.

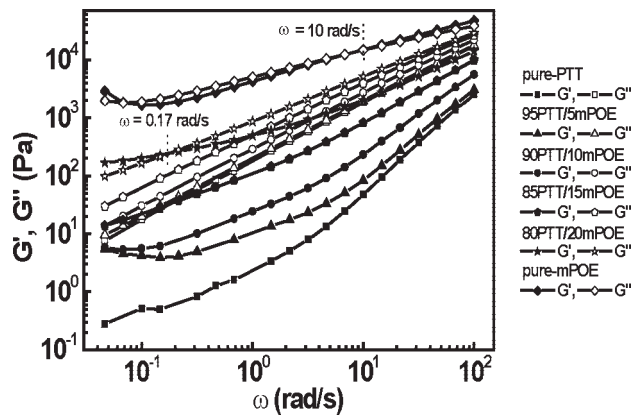
Because  $G''$  was not sensitive to droplet deformation, we focus our discussion on  $G'$ . Figure 3 shows the dependence of  $G'$  and  $G''$  on frequency for each pure component and their blends at  $245^\circ\text{C}$ . When the mPOE content was lower than 5 wt %, the  $G'$ - $\omega$  curves (where  $\omega$  is the angular frequency) of the blends almost overlapped with the curve of the pure PTT in the high-frequency region; this indicated that the viscoelastic properties of the blending samples were predominantly determined by the polymer matrix [see Fig. 3(a)]. For the blending systems, an upturn appeared in the  $G'$ - $\omega$  curves in the low-frequency region; this is called a *second plateau* in rheology. For the blending systems, the second plateau appeared in each  $G'$ - $\omega$  curve in the low-frequency region; this was considered to be the result of the formation of the ordered structure/morphology induced by the aggregation of the elastomer and the phase separation of the blends.<sup>27</sup> Moreover,  $G'$  increased with increasing mPOE content; this resulted from a greater number of crosslinks formed in the mPOE-rich system at a constant frequency.<sup>26</sup> The same trend of  $G''$ - $\omega$  curves is shown in

Figure 3(b). However, the terminal plateau was not clear, except that of mPOE.

Furthermore, the correlation between  $G'$  and  $G''$  for PTT, mPOE, and their blends at  $245^\circ\text{C}$  was investigated in detail. As shown in Figure 4, for PTT and the blends (mPOE content  $<20\%$ ),  $G''$  was always higher than  $G'$  over the entire frequency range examined, which suggested that the disentanglement processes were faster than the entanglement processes for the molecular chains so that the blends always exhibited a predominantly viscous behavior over the whole frequency range studied.<sup>24</sup> However, when the content of mPOE in the blends was larger than 20%, the samples showed a crossover between  $G'$  and  $G''$ , which indicated that  $G''$  was lower at low frequencies, whereas  $G''$  was higher than  $G'$  at higher frequencies. Moreover, the crossover frequency shifted to high frequency with a rise in the content of mPOE. For example, it was 0.17 for the 80PTT/20mPOE blend and 10 for pure mPOE. This result may have been due to the long and flexible



**Figure 3**  $\omega$  dependence of the dynamic modulus [(a)  $G'$ - $\omega$  and (b)  $G''$ - $\omega$ ] for the PTT/mPOE blends at  $245^\circ\text{C}$ : (1) 100/0, (2) 95/5, (3) 90/10, (4) 85/15, (5) 80/20, and (6) 0/100 w/w.



**Figure 4**  $G'$  and  $G''$  as functions of  $\omega$  for the pure components (PTT and mPOE) and their blends at 245°C.

molecular chains of the grafted POE, which could become entangled among themselves and also with the PTT chains.

The modulus was not only related to the content of mPOE but also to the flow temperature. Figure 5 shows the dependence of  $G'$  and  $G''$  on  $\omega$  for the

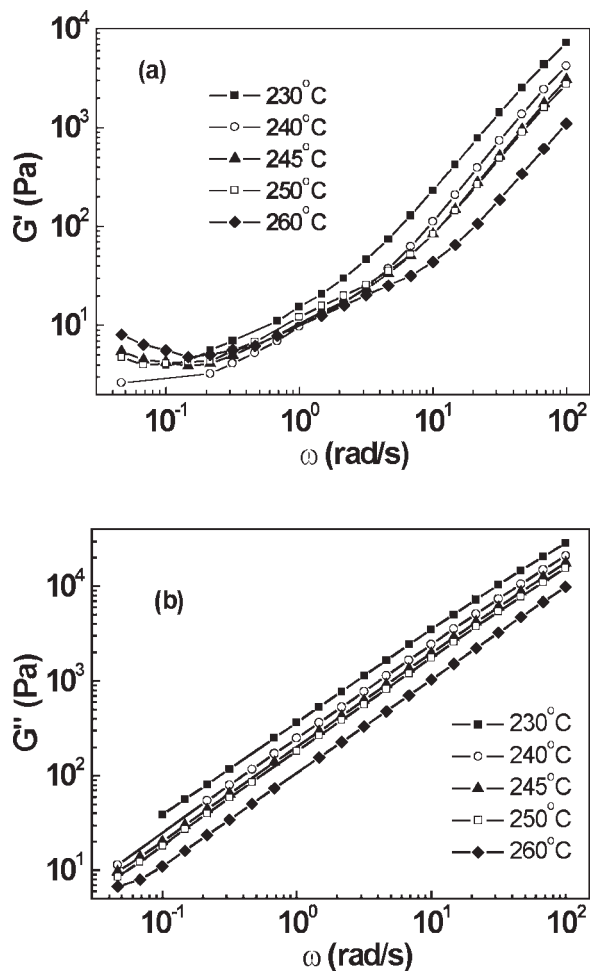


**Figure 5**  $\omega$  dependence of the modulus of PTT/mPOE (95/5 w/w) at different temperatures: (a)  $G'$ - $\omega$  and (b)  $G''$ - $\omega$ .

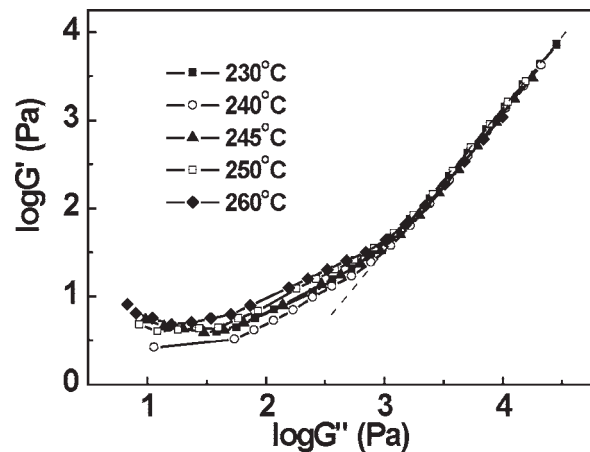


**Figure 6** Han plots of the PTT/mPOE blends (95/15 w/w) at different temperatures.

PTT/mPOE (95/5 w/w) blend at various temperatures. It was obvious that the  $G'$ - $\omega$  curves [see Fig. 5(a)] deviated from the linearity at the low-frequency region. This appearance implied that a change from a homogeneous to heterogeneous structure took place in the blending system.<sup>20</sup> Moreover, the deviation became more pronounced as the temperature increased, except at 240°C. The lowest deviation from linearity at 240°C suggested maximum miscibility at this temperature. However, compared to the shape of the  $G'$ - $\omega$  curves, the shape of the  $G''$ - $\omega$  curves [see Fig. 5(b)] changed very mildly, which indicated that compared with  $G'$ ,  $G''$  was less sensitive to the change in the phase morphology of the polymer blends.

To further study the phase behavior of these binary polymer blends, there was an alternative method suggested by Han to plot  $\log G'$ - $\log G''$ , that is, the Han plot. For temperatures in the phase-separated regime, the Han plot deviates from the master curves.<sup>28</sup> As illustrated in Figure 6, in the low-frequency region, the heterogeneous phase curves for the low-frequency regime deviated from the master curves. Among the five curves, the one at 240°C deviated the least; this indicated that 240°C was the best processing temperature because of the least

**TABLE I**  
Flow Activation Energy for the PTT/mPOE Blends at Different Frequencies

PTT/m POE (w/w)	Activation energy (kJ/mol)				
	100 rad/s	31.6228 rad/s	10 rad/s	4.64159 rad/s	0.1 rad/s
100/0	40.68	43.2	44.49	44.57	26.47
95/5	34.36	37.03	38.68	38.99	36.36
90/10	34.62	38	40.29	40.78	37.76
85/15	32.08	35.44	36.99	37.63	33.18
80/20	30.32	32.84	33.81	34.19	22.96
0/100	24.83	28.71	32.38	34.82	25.09



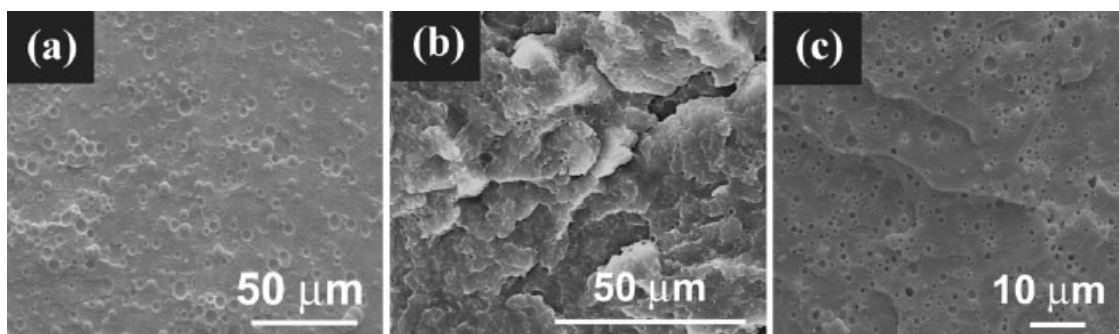


**Figure 7** SEM micrographs of cryofractured surfaces of the PTT/elastomer blends (85/15 w/w): (a) PTT/POE, (b) PTT/mPOE, and (c) xylene-solvent-immersed PTT/mPOE.

phase separation. Although there still existed the contention for using the rheological data to infer the miscibility of polymer blends, the results in this study are also a beneficial reference for the application of the rheological data in deducing the miscibility of polymer blends.

A careful examination of Figure 1 indicates that the dependence of viscosity on frequency was less pronounced for PTT than for mPOE. This kind of dependence can be reflected by the flow activation energy deduced from the Arrhenius equation:

$$\eta = A e^{E_a/RT}$$

where  $\eta$  is the viscosity,  $A$  is the pre-exponential factor,  $E_a$  is the activation energy,  $R$  is the gas constant, and  $T$  is the temperature. Table I shows the effects of mPOE content on the activation energy of the pure polymers and their blends at different frequencies. For all of the blends and pure components, the activation energy of flow at high frequencies was smaller than that at lower frequencies. In addition, PTT possessed a much larger flow activation energy than mPOE. This implied that the viscosity of PTT was not sensitive to the frequency but relied strongly on the temperature; whereas the opposite pattern was observed for mPOE.<sup>29,30</sup> The reason was that the polarity of PTT was greater than that of mPOE. The rigid segments and polar molecular chains of PTT resulted in a great interaction among the PTT molecular chains. Meanwhile, the addition of mPOE into PTT decreased the activation energy of flow. However, the composite containing 10 wt % mPOE had the largest activation energy of flow, which indicated maximum miscibility in this blending system. Similar results have been obtained for ethylene-acrylic acid copolymer (EAA)/ethylene vinyl acetate copolymer (EVA) systems.<sup>29,30</sup>

#### Morphology and interfacial tension of PTT/mPOE

To verify the effect of mPOE on the viscoelastic properties of PTT and the reaction between mPOE

and PTT, a comparison between the morphology of grafted-POE and ungrafted-POE toughened PTT blends was illustrated by SEM. Figure 7 shows the SEM micrographs of the cryofractured surfaces of the PTT/POE and PTT/mPOE blends. In both blends, the compatibilizer content was 15 wt %. As clearly shown in Figure 7(a), the size of the ungrafted POE particles was rather large. Upon fracture, the POE particles were pulled off of the PTT matrix and left many round holes, which had a smooth surface. In addition, the particle size distribution of POE in the PTT matrix was rather broad (from 1.7 to 7.0  $\mu\text{m}$ ). It indicated that the PTT/POE binary blends exhibited poor interfacial adhesion because of poor interaction. A similar result was reported in PET/POE blends.<sup>12</sup> Compared with PTT/POE, PTT/mPOE displayed a significantly finer morphology. As illustrated in Figure 7(b), it was apparent that the fracture surface was rough, and few cavities were observed; this implied that a remarkable compatibilization effect existed between mPOE and PTT. To further investigate the morphology of mPOE in PTT, the impact modifier (mPOE) was extracted by the immersion of the PTT/mPOE

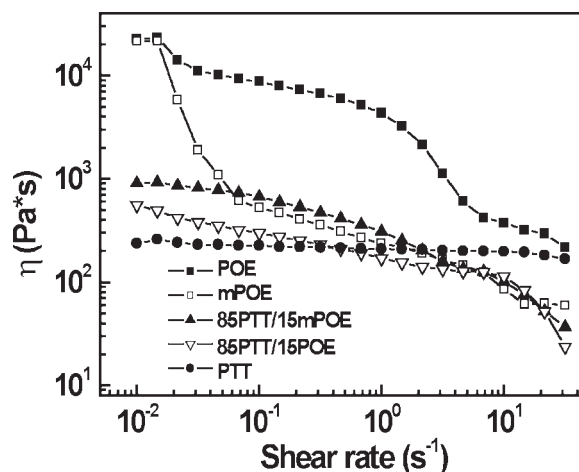


**Figure 8** Relationship of the apparent viscosity ( $\eta$ ) and shear rate for POE, mPOE, PTT, and the PTT blends at 245°C.

TABLE II  
Interfacial Tension Calculation Based on Equation (1)

PTT blend (w/w)	Shear rate (s <sup>-1</sup> )	Average particle diameter (μm)	Toughener viscosity (Pa s)	Matrix viscosity (Pa s)	Toughener viscosity/matrix viscosity	Interfacial tension (mN/m <sup>2</sup> )
85PTT/15mPOE	1	0.07	1327.42	209.03	6.35	0.77
85PTT/15POE	1	3.63	4321.85	209.03	20.68	14.89

blend sample in xylene solvent for about 48 h at 138°C (its boiling point). The holes shown in the PTT matrix [see Fig. 7(c)] revealed that the mPOE particles were fairly small (0.03–0.22 μm) and that mPOE was uniformly dispersed in the PTT matrix. This result further confirmed the lower interfacial energy due to the strong reactions between the dispersed phase and the matrix phase, as shown in the former reaction schemes (Fig. 2).

In polymer blends, the morphology of the phase is strongly related to the interfacial tension and melting viscosity. To obtain a good understanding of the viscoelastic behavior and morphology of the PTT/mPOE systems, the steady rheological behavior was also investigated. Figure 8 shows the steady rheological curves of the POE, POE-g-MAH, PTT, and PTT blends. The following results were found:

1. The apparent viscosity of mPOE was higher than that of POE because of the crosslinking of molecular chains in mPOE.
2. Compared to pure PTT and all of the binary blends, the viscosities of both POE and mPOE were relatively higher.
3. The higher the shear rate was, the lower the viscosities of POE and mPOE were.

However, the effect of shear rate on the viscosity of PTT and all binary blends was found to be insignificant, which was attributed to the hard molecular segments in PTT.

As mentioned in the Introduction, for thermoplastic crystalline polymer and elastomer blends, the size and shape of the dispersed phase and its interaction with the matrix polymer were important factors in the determination of the mechanical performance, and they depended on the chemical components, their melt viscosities, and the extrusion conditions.<sup>12</sup> The relationship between these important parameters, including the interfacial tension ( $\gamma$ ), matrix ( $\eta_m$ ) and rubber ( $\eta_r$ ) melt viscosities, average particle diameter ( $d$ ), and shear rate in the extruder ( $G$ ), is given in the following empirical equation<sup>31</sup>:

$$G\eta_m d/\gamma = 4(\eta_r/\eta_m)^\beta \quad (1)$$

where  $\beta$  is a coefficient with a value of 0.84 when  $\eta_r/\eta_m$  is greater than 1 and  $-0.84$  when  $\eta_r/\eta_m$  is less than 1.

On the basis of Eq. (1), the interfacial tension was calculated with the results of the rheological testing of the components and the morphological characterization of the blends (shown in Table II). Compared with the PTT/POE blend, the PTT/mPOE blend exhibited stronger interactions in the interface and a particularly lower interfacial tension. This result, of course, was mainly attributed to the reactivity of mPOE with PTT, which led to the formation of graft copolymers acting as compatibilizers.

## CONCLUSIONS

The dynamic viscoelastic properties of PTT and its impact-modified PTT/mPOE composites were studied. The flow behavior of the PTT/mPOE blends was affected extensively by the following factors: mPOE concentration and flow temperature. The viscosity of the PTT/mPOE blends was found to be larger than that of PTT alone, which was attributed to coalescence of the particle domains and agglomerates. The blends had the largest flow activation energy when the mPOE content was 10 wt %. Also, the blends had the best miscibility at a flow temperature of 240°C. On the other hand, the morphology study indicated that the MAH grafting of POE resulted in a significant improvement in the compatibility and interfacial adhesion between PTT and POE and a sharp reduction in the mPOE particle size and interface tension between mPOE and PTT. Furthermore, the MAH content in POE probably affected the viscoelastic properties of the blends. Further studies on this aspect are being carried out in our laboratory.

## References

1. Kim, K. J.; Bae, J. H.; Kim, Y. H. *Polymer* 2001, 42, 1023.
2. Wu, G.; Li, H. W.; Wu, Y. Q.; Cuculo, J. A. *Polymer* 2002, 43, 4915.
3. Chang, J.-H.; Kim, S. J.; Im, S. *Polymer* 2004, 45, 5171.
4. Brown, H. S.; Chuah, H. H. *Chem Fibers Int* 1997, 47, 72.
5. Chiu, H. J.; Huang, J. M. *J Appl Polym Sci* 2006, 99, 2421.
6. Aravinda, I.; Alberta, P.; Ranganathaiah, C.; Kurianb, J. V.; Thomas, S. *Polymer* 2004, 45, 4925.
7. Ravikumar, H. B.; Ranganathaiah, C. *Polym Int* 2005, 54, 1288.
8. Ravikumar, H. B.; Ranganathaiah, C.; Kumaraswamy, G. N.; Thomas, S. *Polymer* 2005, 46, 2372.

9. Ravikumar, H. B.; Ranganathaiah, C.; Kumaraswamy, G. N.; Deepa Urs, M. V.; Jagannath, J. H.; Bawa, A. S.; Thomas, S. *J Appl Polym Sci* 2006, 100, 740.
10. Krutphun, P.; Supaphol, P. *Eur Polym J* 2005, 41, 1561.
11. Huang, D. H.; Woo, E. M.; Lee, L. T. *Colloid Polym Sci* 2006, 284, 843.
12. Chiu, H. T.; Hsiao, Y. K. *J Polym Res* 2005, 12, 355.
13. Chiu, H. T.; Hsiao, Y. K. *Polym Eng Sci* 2004, 44, 2340.
14. Silva, A. L. N.; Rocha, M. C. G.; Coutinho, F. M. B. *Polym Test* 2002, 21, 289.
15. Guerrica-Echevarría, G.; Eguiazábal, J. I.; Nazábal, J. *Eur Polym J* 2007, 43, 1027.
16. Aróstegui, A.; Gaztelumendi, M.; Nazábal, J. *Polymer* 2001, 42, 9565.
17. Wu, G.; Song, Y. H.; Zheng, Q.; Du, M.; Zhang, P. J. *J Appl Polym Sci* 2003, 88, 2160.
18. Nesarikar, A. R. *Macromolecules* 1995, 28, 7202.
19. Kapnistos, M.; Hinrichs, A.; Vlassopoulos, D.; Anastasiadis, S. H.; Stammer, A.; Wolf, B. A. *Macromolecules* 1996, 29, 7155.
20. Zheng, Q.; Du, M.; Yang, B. B.; Gang, W. *Polymer* 2001, 42, 5743.
21. Chopra, D.; Kontopoulou, M.; Vlassopoulos, D.; Hatzikiriakos, S. G. *Rheol Acta* 2002, 41, 10.
22. Han, C. D.; Baek, D. M.; Kim, J. K.; Ogawa, T.; Sakamoto, N.; Hashimoto, T. *Macromolecules* 1995, 28, 5043.
23. Graebing, D.; Muller, R.; Palierne, J. F. *Macromolecules* 1993, 26, 320.
24. Yang, J.; Chen, X. D.; Fu, R. W.; Zhang, M. Q.; Chen, H. B.; Wang, J. S. *J Appl Polym Sci* 2008, 109, 3452.
25. Jafaria, S. H.; Pötschke, P.; Stephana, M.; Warthb, H.; Alberts, H. *Polymer* 2002, 43, 6985.
26. Steinmann, S.; Gronski, W.; Friedrich, C. *Rheol Acta* 2002, 41, 77.
27. Zheng, Q.; Cao, Y. X.; Du, M. *Chin J Polym Sci* 2004, 22, 363.
28. Huang, Y. J.; Jiang, S. J.; Li, G. X.; Chen, D. H. *Acta Mater* 2005, 53, 5117.
29. Siddaramaiah; Bhattachary, A. K.; Nando, G. B. *J Appl Polym Sci* 2005, 98, 1947.
30. Wang, X. D.; Luo, X. *Eur Polym J* 2004, 40, 2391.
31. Wu, S. H. *Polymer* 1985, 26, 1855.